



OPEN

Association mapping of autumn-seeded rye (*Secale cereale* L.) reveals genetic linkages between genes controlling winter hardiness and plant development

Monica Båga¹, Hirbod Bahrani¹, Jamie Larsen², Bernd Hackauf³, Robert J. Graf⁴, Andre Laroche⁴ & Ravindra N. Chibbar¹✉

Winter field survival (WFS) in autumn-seeded winter cereals is a complex trait associated with low temperature tolerance (LTT), prostrate growth habit (PGH), and final leaf number (FLN). WFS and the three sub-traits were analyzed by a genome-wide association study of 96 rye (*Secale cereale* L.) genotypes of different origins and winter-hardiness levels. A total of 10,244 single nucleotide polymorphism (SNP) markers were identified by genotyping by sequencing and 259 marker-trait associations (MTAs; $p < 0.01$) were revealed by association mapping. The ten most significant SNPs ($p < 1.49e-04$) associated with WFS corresponded to nine strong candidate genes: *Inducer of CBF Expression 1 (ICE1)*, *Cold-regulated 413-Plasma Membrane Protein 1 (COR413-PM1)*, *Ice Recrystallization Inhibition Protein 1 (IRIP1)*, *Jasmonate-resistant 1 (JAR1)*, *BIPP2C1-like protein phosphatase*, *Chloroplast Unusual Positioning Protein-1 (CHUP1)*, *FRIGIDA-like 4 (FRL4-like) protein*, *Chalcone Synthase 2 (CHS2)*, and *Phenylalanine Ammonia-lyase 8 (PAL8)*. Seven of the candidate genes were also significant for one or several of the sub-traits supporting the hypothesis that WFS, LTT, FLN, and PGH are genetically interlinked. The winter-hardy rye genotypes generally carried additional allele variants for the strong candidate genes, which suggested allele diversity was a major contributor to cold acclimation efficiency and consistent high WFS under varying field conditions.

Rye (*Secale cereale* L.) is a member of the *Triticeae* tribe within the *Pooideae* subfamily, which belongs to the *Poaceae* grass family. Similar to the *Triticeae* crops barley (*Hordeum vulgare* L.) and bread wheat (*Triticum aestivum* L.), rye is mainly cultivated for its grain, but can also be grown for its biomass used as forage or production of bioenergy. The main rye producing areas are located in North America, China, Russia, and Europe, where the grain is used for production of bread, alcoholic beverages, and feed¹.

The *Triticeae* genomes are likely derived from a common progenitor genome which explains the high sequence synteny between the seven chromosomes of the diploid rye R genome ($2n = 2x = 14$), diploid H genome of barley and the three genomes (A, B, D) of hexaploid wheat². Since the wheat and rye lineages diverged, several translocations have occurred within the rye genome as revealed by transcript mapping and genome sequence assemblies²⁻⁴. The haplotype diversity in rye is high⁵ as it is an open-pollinated species, whereas current wheat and barley cultivars have lower genetic diversity due to self-pollination and extensive breeding during the last century. Although some genetic erosion has occurred in improved rye germplasm, the landraces and wild rye lines display a relatively high allelic variation that is available for mining⁶.

Rye can serve as a good model for winter hardiness studies in *Triticeae* species, as many autumn-seeded rye varieties developed for northern latitudes have the highest winter-hardiness among cereal crops⁷. Most of the temperate grasses are inherently chilling tolerant, but acquire frost tolerance following weeks of acclimation to low but non-freezing temperatures⁸. For autumn-seeded cereals, the cold acclimation process occurs prior to

¹Department of Plant Sciences, University of Saskatchewan, Saskatoon, SK S7N 5A8, Canada. ²Harrow Research and Development Centre, Agriculture and Agri-Food Canada, Harrow, ON N0R 1G0, Canada. ³Institute for Breeding Research on Agricultural Crops, Julius Kühn-Institut, 18190 Sanitz, Germany. ⁴Lethbridge Research and Development Centre, Agriculture and Agri-Food Canada, Lethbridge, AB T1J 4B1, Canada. ✉email: ravi.chibbar@usask.ca

winter and is characterized by two major physiological processes: (a) accumulation of increased freezing tolerance and (b) fulfilment of vernalization requirement causing shift from vegetative to reproductive growth at the shoot apical meristem (SAM). Upon vernalization saturation, further development of floral organs is paused until new growth from the crown tissue is stimulated by inductive photoperiod and temperature in the spring⁹.

Cold acclimation initiates when plants integrate and respond to environmental signals received from gradual reductions in photoperiod, daily temperature, light intensity, and red/far-red ratio in incoming light^{10,11}. An early start and long acclimation period result in higher winter hardiness for winter cereals, and thus, the timing of floral transition impacts the total amount of accumulated freezing tolerance¹². Cold acclimated cereals further increase their freezing tolerance when exposed to slightly below 0 °C temperatures, which stimulate a second hardening process¹³. Transcriptional analyses show different sets of genes are induced during the above-zero and sub-zero cold hardening processes¹⁴.

Winter-hardy plants undergo a multitude of developmental adjustments during cold acclimation to build up frost resistance⁸. The morphological changes observed in cereals generally include a switch to prostrate growth habit (PGH), compact growth, strengthening of cell walls, changes in membrane structures, and increased number of leaf initials formed at SAM^{12,15–18}. The biochemical changes involve production of various cryoprotectants, antioxidants, and antifreeze proteins to aid protection against future frost damage^{19,20}. An enhanced photosynthetic performance is observed for the most winter-hardy cereals and results in higher biomass production and reduced susceptibility to photoinhibition as compared to tender genotypes²¹. Through the modification of photosynthesis, winter-hardy cereals can effectively increase their carbon pools in crown tissues to be retrieved during deacclimation incidents throughout winter and regrowth in the spring. Cold acclimation also causes epigenetic changes at the DNA and histone levels with effects on gene activities^{22,23}. Overall, cold responses are coordinated by an extensive cross-talk between cold-induced Ca²⁺, reactive oxygen species, phytohormone, and light signaling pathways^{10,24–26}, of which retrograde/antegrade stress signaling between plastids and nucleus are suggested to play a central role^{15,27}.

The *Vernalization 1 (VRN1)* and *Frost resistance-2 (FR-2)* loci on homoeologous group 5 chromosomes are the major determinants for freezing tolerance in *Triticeae* species²⁸. Allelic differences at *VRN1*, *Fr-A2* and their interactions relate to cold acclimation efficiency and duration²⁹. In addition, *VRN1* and *FR-2* interactions with genes controlling plant development is required for optimal cold acclimation^{12,30,31}. Large clusters of *AP2/ERF* transcription factor genes denoted *C-repeat Binding Factors (CBFs)* are present at *FR* loci, where variations in *CBF* expression levels, copy numbers, and haplotypes affect freezing tolerance and WFS levels in hexaploid wheat^{32,33}, barley³⁴ and rye^{35,36}. Cold-induced CBFs bind to *C-repeat/dehydration-responsive* elements present in promoters of many cold-regulated (*COR*) genes and thereby induce their expression during cold stress³⁷. Besides the *CBF-COR* regulon, additional pathways respond to cold stress³⁸ as demonstrated by triple *CBF* mutants in *Arabidopsis* showing reduced frost tolerance but retained cold-response for several *COR* genes³⁹.

In a previous study, we analyzed WFS in a rye population of 96 genotypes of different origins and winter hardiness levels and showed WFS was almost entirely determined by the cold acclimation process⁴⁰. In addition, the developmental traits FLN and PGH were highly correlated with both WFS and LTT ($r = 0.59–0.80$; $p < 0.001$). Estimations of heritability for WFS, FLN and PGH revealed moderate to high values ($h^2 = 0.45$ to 0.81), which allowed us in this study to perform a genome-wide association study (GWAS) with the aim to find genes influencing WFS and associated traits. GWAS is useful for identification of candidate genes for traits showing variation in a population of unrelated genotypes⁴¹. The genetic mapping technology has greatly benefitted from recently developed next generation sequencing and genotyping by sequencing (GBS) technologies, which allow identification of large numbers of single nucleotide polymorphism (SNP) markers⁴². Rye is well suited for association mapping as it's out-crossing nature generates a low linkage disequilibrium (LD)⁵. In addition, a near full-length annotated genome (6.74 Gb of estimated 7.9 Gb) sequence is available for genome mapping⁴. The association study of rye genotype panel revealed several candidate genes were shared between WFS and one or more of the three associated traits; thus, suggesting the traits were genetically interconnected. The characteristics of nine strong candidate genes affecting WFS are discussed.

Materials and methods

Plant materials. Rye (*Secale cereale* L.) accessions (96 genotypes) used for association mapping are listed in Table S1 and were phenotyped in a separate study⁴⁰. The genotypes were maintained through generations by crossing five plants per pollination bag. All experimental research and field studies on plants (cultivated or wild) including collection of plant material complied with the institutional and funding agencies, national and international guidelines and legislation. The permission to collect seeds and plant material was granted under the material transfer agreements with international gene banks and Universities.

Field trials to determine WFS. Five years (2014–2019) of field trials were conducted at the University of Saskatchewan Experimental Farm, Saskatoon, Saskatchewan, Canada (52° 10' N, 106° 30' W, and 457 m altitude) as previously reported⁴⁰. Briefly, the genotypes were seeded in early September with each genotype randomly placed in three 3.6 m rows, 100 seeds/row, and 30 cm row spacing. For each genotype and trial, the germination frequency was determined 6 weeks upon seeding and survival frequency was determined the following spring. The genotypes survival frequencies from the trials were used to calculate the Best Linear Unbiased Estimates (BLUEs)⁴³ for WFS for each genotype using the statistical analysis Multi Environment Trial Analysis with R (META-R) software version 6.04 (CIMMYT Research Data & Software Repository Network, Mexico). Based on the BLUE scores, WFS for the population was divided into five groups: very high (64.5–92.5%; 19 genotypes), high (56.7–64.3%; 20 genotypes), moderate (46.2–56.6%; 19 genotypes), low (30.5–43.7%; 19 genotypes) and very low (0–25.2%; 19 genotypes) WFS (Table S1).

Freeze tests to determine LTT. Freeze tests of cold acclimated plants were performed by a step wise decrease in temperature using an EPZ-4H test chamber (ESPEC North America Inc., Hudsonville, MI, USA) as described⁴⁰. The freezing temperature at which 50% of the plants regrew two weeks upon exposure to freezing was noted as the LT_{50} temperature. Negative LT_{50} values represented the LTT score.

Assessment of plant developmental traits. The two developmental traits PGH and FLN were analyzed in four separate trials with five plants per genotype in each trial as previously described⁴⁰. PGH was rated upon completion of cold-acclimation in growth chamber. The visual PGH rating was based on three types of growth habits: (1) erect, (2) intermediate, and (3) prostrate. To determine FLN, plant leaves were labeled numerically as they developed from the primary stem. The flag leaf number was recorded as FLN. BLUE scores for the two developmental traits were calculated to determine the overall FLN and PGH scores for each genotype.

DNA extraction and GBS analysis. Leaf tissue (~130 mg) was collected from five two-week-old plants of each genotype and ground to a fine powder in liquid nitrogen using a mortar and pestle. DNA was extracted from the homogenized leaf material using a standard hexadecyltrimethylammonium bromide-based method. The concentration of isolated DNA was determined using a Quant-iT™ PicoGreen® dsDNA Assay Kit (Invitrogen, Molecular Probes, Eugene, OR, USA). Uniform presence of high molecular weight DNA in the samples was confirmed by agarose (0.8%) gel electrophoresis. Normalized DNA preparations at $10 \text{ ng } \mu\text{L}^{-1}$ (20 μL in total) were subjected to library preparations and GBS analysis, a service provided by Plateforme d'analyses Génomiques of the Institut de Biologie Intégrative et des Systèmes (IBIS), Université Laval, Québec, Canada. Reduced-representation libraries were prepared from *Pst*I and *Msp*I double-digested DNA as described⁴⁴ using an Ion CHEF System, Hi-Q reagents, and P1 V3 chips (ThermoFisher Scientific, Life Technologies Inc., ON, Canada) for the library and chip preparations⁴⁵. Sequencing analysis was done on an Ion Proton Sequencer (ThermoFisher Scientific, Life Technologies Inc., Waltham, MA, USA).

SNP calling. Raw FASTQ files obtained from GBS analyses of the 96 rye genotypes were processed by Trimmomatic version 0.36⁴⁶ with a four-base window setting and a minimum average quality score of 16. Barcodes, adaptors, and reads less than 36 bp were eliminated from the sequences before alignment to scaffold sequences of rye inbred line Lo7–version 2³ using Bowtie 2.0 version 2.2.6 software⁴⁷. Duplicates were removed using the `rmDup` function⁴⁸ and SNP variants including insertions/deletions (InDels) were detected by Sequence Alignment/Map tools version 0.1.19⁴⁸. The markers were filtered using the Variant Call Format tool version 0.1.14⁴⁹, a minor allele frequency > 5%, and a minimum reading depth of 6.0. A total of 10,244 SNP markers were identified and numbered according to matching scaffold of rye inbred line Lo7–version 2³. The selected markers contained no missing data. BLASTn analyses against the 2021 rye Lo7 v1 genome assembly⁴ were done using default settings and e-value threshold set to $\leq 1e-70$. SNP marker distances and squared correlations of allele frequencies (r^2) for 9547 mapped markers for the population were determined by the TASSEL version 5.2.20 software⁵⁰. The generated data was displayed as linkage disequilibrium (LD) decay plots using the RStudio package version 3.5.1 software⁵¹. LD value at $r^2 = 0.20$ was estimated from each plot's trend line.

Analyses of population structure. The genetic relationship among the 96 rye genotypes was analyzed using a model-based clustering method implemented by the STRUCTURE version 2.3.4 software⁵². The analysis was made using genetic information for all 10,244 SNP markers. Based on an admixed model and allele frequencies correlated, the number of subpopulations (K) ranging from 1 to 9 were tested with burn-in time set to 50,000 and Markov Chain Monte Carlo replication number to 100,000. A total of 20 runs were performed for each data set to compute the log likelihood for each simulated K value. The STRUCTURE HARVESTER version 0.6.94 software⁵³ was used to establish the optimal number of sub-populations according to the ΔK method⁵⁴.

To visualize the relative genetic distances between the rye genotypes, the SNP data was subjected to a principal component analysis (PCA) conducted using RStudio package version 3.5.1 software⁵⁵. The evolutionary relationships among the rye genotypes were calculated by the centered JBS method provided by the TASSEL version 5.2.20 software^{50,56}, and the result was displayed as a neighbor-joining dendrogram tree.

Marker-trait association (MTA) analysis. Phenotypic data for WFS, LTT, FLN, and PGH of the rye population was determined by replicated trials in a previous study⁴⁰. The population structure obtained from STRUCTURE version 2.3.4, kinship data, genotype, and phenotype data for the rye population were used to determine p and R^2 (explained variation) for MTAs by the mixed linear model available in TASSEL version 5.2.20 software⁵⁰. The minor allele frequency was set to > 5%. Significant SNP variants were initially tested based on a false discovery rate (FDR)-adjusted p value of 0.05 following a step-wise procedure⁵⁷, and lowest adjusted p values (threshold $p < 1.49e-04$) was identified after a Bonferroni correction⁵⁸. To illustrate the relationships between the allele variations and trait values for the 96 genotypes, phenotype and genotype data for the population was subjected to a principal component analysis (PCA) using RStudio package version 3.5.1 software⁵⁵. The results of the analyses were displayed as bi-plots.

Prediction of candidate genes. The marker sequences carrying SNP of interest underwent BLASTn searches (default settings) against the *Secale cereale* Lo7 version 1 pseudomolecules hosted by Graingenes (<https://wheat.pw.usda.gov/blast/>) and the IPK Galaxy Blast Suite (<https://galaxy-web.ipk-gatersleben.de>) databases to identify matches to the latest assembly of rye Lo7 genome and its annotated genes⁴. BLAST searches were also made against the National Center for Biotechnology Information database (<https://blast.ncbi.nlm.nih>).

gov). Gene orthologues in hexaploid wheat were identified by BLAST searches against the EnsemblPlants (<http://plants.ensembl.org>) wheat RefSeqv2.0 assembly constructed by the International Wheat Genome Sequencing Consortium⁵⁹. The DNASTAR software package version 15.3.0 (DNASTAR, Madison, WI, USA) was used to analyze gene sequences. A physical map of rye was drawn using the MapChart software version 2.3⁶⁰. Transmembrane, signal peptide and phosphorylation site predictions in proteins were done using TMHMM, SignalP 5.0, and NetPhos 3.1 programs available at <https://services.healthtech.dtu.dk/>.

Consent for publication. The manuscript was reviewed, edited by all authors and approved for submission.

Results

Structure analysis of GBS data generated for rye population. The GBS analysis generated a total of 357.1 million reads with an average read length of 108 nucleotides. Alignment of the processed sequences to scaffold sequences of rye inbred line Lo7 genome version 2³ produced 252,158 SNP markers, of which 10,244 SNP markers with no missing data remained upon data filtering. BLASTn analyses of the marker sequences to the 2021 rye genome assembly⁴ assigned a total of 9,547 markers (93.2%) to chromosome positions. The markers were relatively evenly distributed on the genome, with an average of 1364 markers per chromosome (Table S2). Estimations of LD yielded values between 3428 and 5153 bp for the individual chromosomes and an average of 4266 bp for the whole genome (Table S2; Fig. S1). With relatively low LD values, the mapping data was considered suitable for association mapping.

The SNP data was analyzed by PCA, which showed the first and second coordinates explained 3.6% and 2.3% of the total genetic variation, respectively (Fig. 1). Three clusters were distinguished from the PCA plot, where the largest cluster (II) with 63 genotypes contained several genotypes with the highest WFS scores, but also relatively cold-sensitive genotypes such as Petkus and Carsten (Fig. 1; Table S1). Like cluster II, cluster I with 28 genotypes included several very winter-hardy genotypes intermingled with tender genotypes. Cluster III consisted mainly of perennial types with relatively low WFS scores. The existence of three subpopulations was also supported by a STRUCTURE HARVESTER analysis, which deduced the maximum value for Delta K to three (Fig. S2). A neighbor-joining phylogenetic tree constructed from the SNP data repositioned the Canadian genotypes Puma, Cougar and Gazelle in PCA cluster I to branch II of the phylogenetic tree (Fig. S3; Table S1). The tree also indicated division of branch II into two sub-branches, where Carsten was placed in branch IIa and Petkus in branch IIb. A separation of Carsten and Petkus into different gene pools can be explained by the use of these genotypes in different breeding programs^{6,61}.

Identification of SNP markers associated with developmental and cold tolerance traits. Association mapping using SNP and trait data for rye population led to identification of 189 SNP marker variations that were significantly ($p < 0.01$) associated with one or several of the WFS, LTT, FLN, and PGH trait values (Table S3). In total, 259 MTAs were identified, where 98 markers associated with WFS, 26 with LTT, 75 with FLN, and 60 with PGH (Table 1). LTT shared most markers with WFS (16 out of 26; 61.5%), followed by FLN (26 out of 75; 34.7%), and PGH (18 out of 60; 30.0%), thus indicating the four traits may be genetically linked with each other.

The SNP markers were divided into two groups based on their significance level (Table S3). Group 1 contained the ten most significant markers, which were distinguished after a Bonferroni correction of mapping data generating a new and more stringent significant p value ($p < 1.49e-04$; FDR < 0.05) (Table 2). A total of 22 MTAs was identified for the group 1 markers, which matched nine candidate genes. The second group included 179 markers ($p < 0.001$), of which 81 matched genes (Table S3). Of the 90 genes associated with MTAs, 32 amino acid substitutions were predicted from the SNP variations. All but five of the 189 SNP markers could be placed on de novo assembled Lo7 physical map of rye⁴ (Fig. 4). Below is a presentation of the nine strongest candidate genes listed in Table 2.

BIPP2C1-like protein phosphatase. The most significant marker identified in the study (Xuos526258) was associated with all four traits, WFS, LTT, FLN, and PGH (Table 2) and matched *SECCE7Rv1G0469720.1*, a PPM-type protein phosphatase 2C gene (*PP2C*) located on chromosome 7R (112,789 Mb; Fig. 4). The predicted rye phosphatase showed highest sequence identity (84.1%) to benzothiadiazole-induced protein phosphatase 2C1 (*BIPP2C1*) from *Triticum dicoccoides* (XP_037426067). BIPP2C1 proteases are members of the Mg^{2+}/Mn^{2+} -dependent Ser/Thr phosphatase family subclade K in *Arabidopsis*, rice, and wheat⁶²⁻⁶⁴. No function has been assigned for wheat BIPP2C1⁶⁴, whereas clade K member OsBIPP2C1/PP45 from rice is cold-induced⁶³, protects against abiotic and biotic stresses⁶⁵, and has a negative role in abscisic acid signaling⁶⁶. The T/G SNP variation for rye *BIPP2C1* caused a V₁₈₅ to G₁₈₅ change within a glycine-rich region located outside of the catalytic domain for the phosphatase (data not shown). All 38 rye genotypes with low or very low WFS encoded only the G₁₈₅ variant for the phosphatase (Table S4), and this allele variant was also associated with low FLN values, low LTT (high LT₅₀ values), and erect growth habit (Fig. 2). Genotypes encoding both (V₁₈₅/G₁₈₅) or only V₁₈₅ variant for BIPP2C1 had overall the highest WFS, LTT and FLN values (Fig. 2; Table S4).

Ice recrystallization inhibition protein 1 (IRIP1). The high-significance marker Xuos530120 associated with WFS, LTT, and PGH (Table 2) was found to match *SECCE7Rv1G0458910.1* located on chromosome 7R (23,476 Mb; Fig. 4). The targeted gene codes for an ice recrystallization inhibition protein 1 (IRIP1), which belongs to a group of proteins only produced by *Pooideae* species⁶⁷. IRIPs carry a N-terminal leucine-rich repeat (LRR) domain, similar to those of phytosulfokine receptor tyrosine kinases, and an ice-binding domain at the

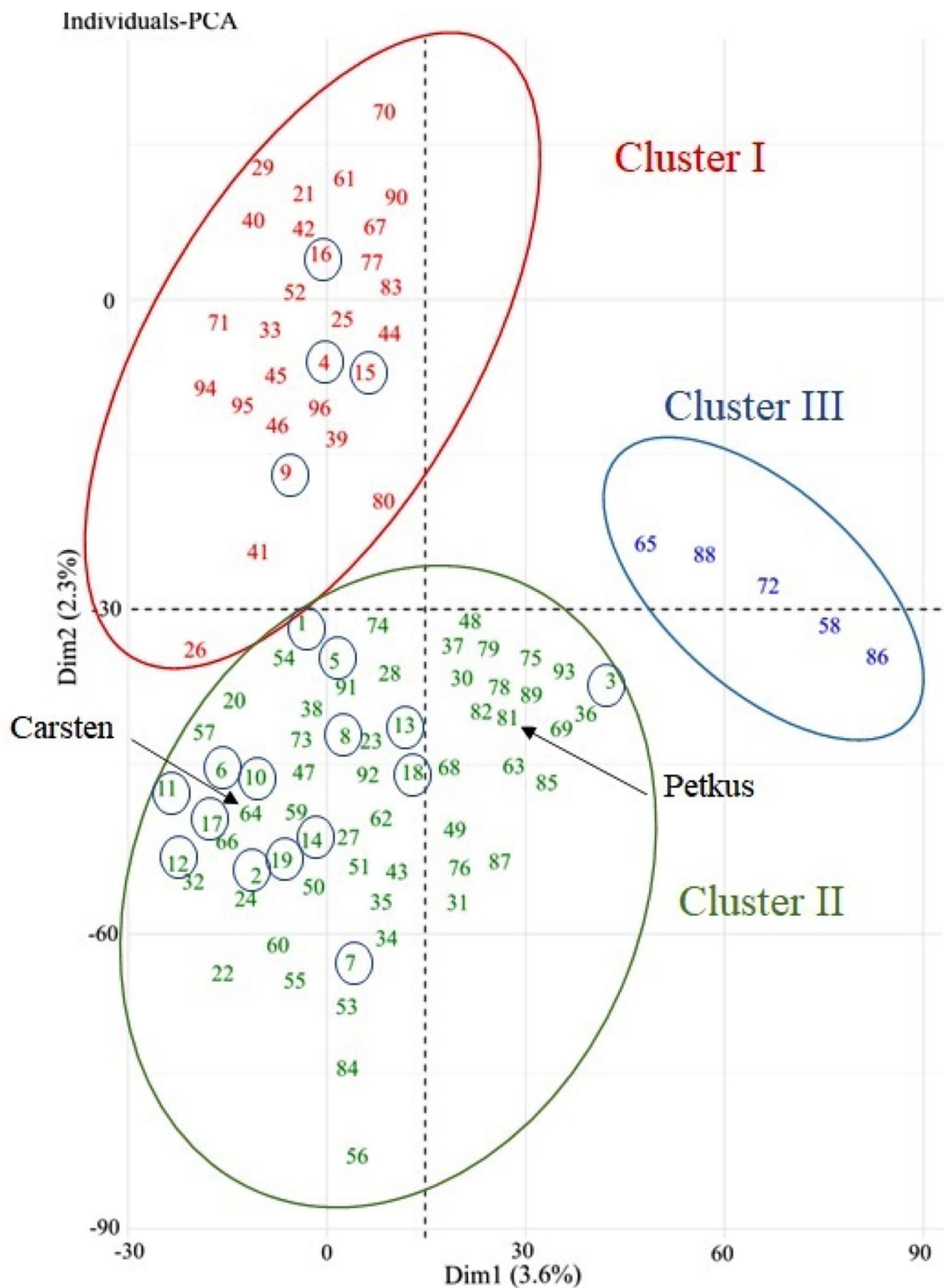


Figure 1. Principal component analysis (PCA) score plot. Plot generated from analysis of 10,244 SNP markers identified in rye population of 96 accessions. The x axis represents the eigenvalue for principal component 1 (PC1) and the y axis for PC2. Genotypes with highest WFS are encircled and arrows refer to less cold hardy Petkus and Carsten, respectively. Data for the individual genotypes is listed in Table S1.

C-terminal end⁶⁸. During exposure to freezing, IRIPs present in the apoplastic space bind to small ice crystals and thereby inhibit further ice recrystallization and frost damage of the plasma membrane^{67,69}. The proteins may also prevent bacteria from serving as ice-nucleators in the extra-cellular space⁷⁰. The Xuos530120 SNP encoded

Trait	Total number of SNPs associated with trait	Number of markers shared		
		LTT	FLN	PGH
WFS	98	16	26	18
LTT	26		9	9
FLN	75			13
PGH	60			

Table 1. Total number and shared SNP markers between traits.

Marker ID ^{1/}	SNP ^{2/}	SNP position (bp) ^{3/}	P value ^{4/}	R ² ^{5/}	MTA	Corresponding gene; protein	Amino acid change
Xuos526258	T/G	Chr7:112,789,055	1.10E-05	20.7	Xuos526258_WFS	SECCE7Rv1G0469720.1;Benzothiadiazole-induced protein phosphatase 2C1 (BIPP2C1)	V/G
			1.50 E-05	18.5	Xuos526258_FLN		
			3.84 E-05	16.4	Xuos526258_PGH		
			4.17 E-05	17.9	Xuos526258_LTT		
Xuos530120	G/C	Chr7:23,476,102	5.66 E-05	14.5	Xuos530120_WFS	SECCE7Rv1G0458910.1;Ice recrystallization inhibition protein 1 (IRIP1)	G/R
			6.62 E-05	16.3	Xuos530120_PGH		
			6.80 E-05	16.2	Xuos530120_LTT		
Xuos615052	T/A	Chr3:937,715,414	7.94 E-05	14.7	Xuos615052_WFS	SECCE3Rv1G0209310.1;Inducer of CBF expression 1 (ICE1)	L/H
			8.06 E-05	15.8	Xuos615052_FLN		
			8.12 E-05	14.7	Xuos615052_PGH		
			1.04 E-04	15.6	Xuos615052_LTT		
Xuos519455	T/A	Chr6:434,208,045	1.10 E-04	13.1	Xuos519455_WFS	SECCE6Rv1G0399250.1;Phenylalanine ammonia lyase 8 (PAL8)	F/I
Xuos613978	A/G	Chr5:727,383,264	1.11 E-04	15.5	Xuos613978_WFS	SECCE5Rv1G0354870.1, SECCE5Rv1G0354880.1;Cold-regulated plasma membrane 413 protein (COR413-PM)	T/A
		Chr5:727,387,758	1.18 E-04	15.3	Xuos613978_FLN		
Xuos75199	A/C	Chr1:716,318,047	1.20 E-04	15.3	Xuos75199_WFS	SECCE1Rv1G0061510.1;Jasmonat E-resistant 1 (JAR1)	N/T
			1.33 E-04	14.6	Xuos75199_FLN		
Xuos76228a	C/G	Chr2:933,364,125	1.39 E-04	14.5	Xuos76228a_WFS	SECCE2Rv1G0140890.1;Chalcone synthase 2 (CHS2)	Q/E
Xuos76228b	C/T	Chr2:933,364,201	1.44 E-04	13.4	Xuos76228b_WFS		A/V
Xuos2264	T/G	Chr1:109,131,359	1.45 E-04	12.5	Xuos2264_WFS	SECCE1Rv1G0013960.1;Chloroplast unusual positioning protein 1 (CHUP1)	None (G/G)
			1.45 E-04	14.4	Xuos2264_PGH		
			1.46 E-04	14.8	Xuos2264_FLN		
Xuos372616	C/A	Chr5:755,939,404	1.47 E-04	14.8	Xuos372616_WFS	FRIGIDA-like 4 (FRL4-like)	None (A/A)

Table 2. Most significant MTAs identified in the study. ^{1/}Number refers to matching rye Lo7_v2_scaffold number^{3/}; ^{2/}Reference/alternative allele; ^{3/}Position on rye Lo7 pseudomolecules version 1 assembly^{4/}; ^{4/}Calculated upon Bonferroni correction. ^{5/}Explained variation.

a G₃₆/R₃₆ variation within one of two preserved cysteine loops preceding the LRR-like region, which may be proteolytically separated from the ice-binding domain in the apoplastic space as suggested by studies in *Brachypodium distachyon*⁶⁹. Thus, the amino acid substitution for the rye IRIP was not expected to influence protein binding to ice crystals, but could affect the function of the N-terminal region (Fig. S4). Almost all genotypes (36 out of 38) with low and very low WFS encoded only the R₃₆ IRIP variant (Table S4), whereas the highest WFS, LTT, and FLN values were favored by the G₃₆ IRIP variant (Fig. 2). Many additional IRIP variants may be produced from the 7R locus as the reference genome carries at least 13 *IRIP*-like coding regions (> 80% nucleotide sequence identity) arranged in tandem with *SECCE7Rv1G0458910*.

Cold-regulated 413 plasma membrane (COR413-PM)-like. One common SNP for WFS and FLN was carried by marker sequence Xuos613978 (Table 2), which showed high sequence identity to two *COR413* genes, *SECCE5Rv1G0354870.1* (89.1%) and *SECCE5Rv1G0354880.1* (89.2%), respectively. The two *COR* genes are arranged in tandem ~ 11 Mb distal of the vernalization locus (*ScVRN1*) on chromosome 5R (727,383 and 727,388 Mb; Fig. 4). *COR413* genes are expressed during cold stress and their expression levels relate to accumulated freezing tolerance in cereals and *Arabidopsis* during cold acclimation^{71,72}. The rye *COR413* proteins encoded from 5R locus were from BLAST and SignalP 5.0 algorithm analyses predicted to be targeted to the plasma membrane (Fig. S4). Additional predictions by TMHMM algorithm supported the N-terminal end of *COR413-PM* encoded by *SECCE5Rv1G0354870.1* was positioned inside of the plasma membrane, whereas the N-terminal end of *COR413-PM* encoded from *SECCE5Rv1G0354880.1* was positioned outside of the plasma membrane (Fig. S4). The Xuos613978 SNP caused a T₃₀ to A₃₀ variation proximal of the first predicted transmembrane region on *COR413-PM*. The SNP variation may involve a possible phosphorylation site at T₃₀ accord-

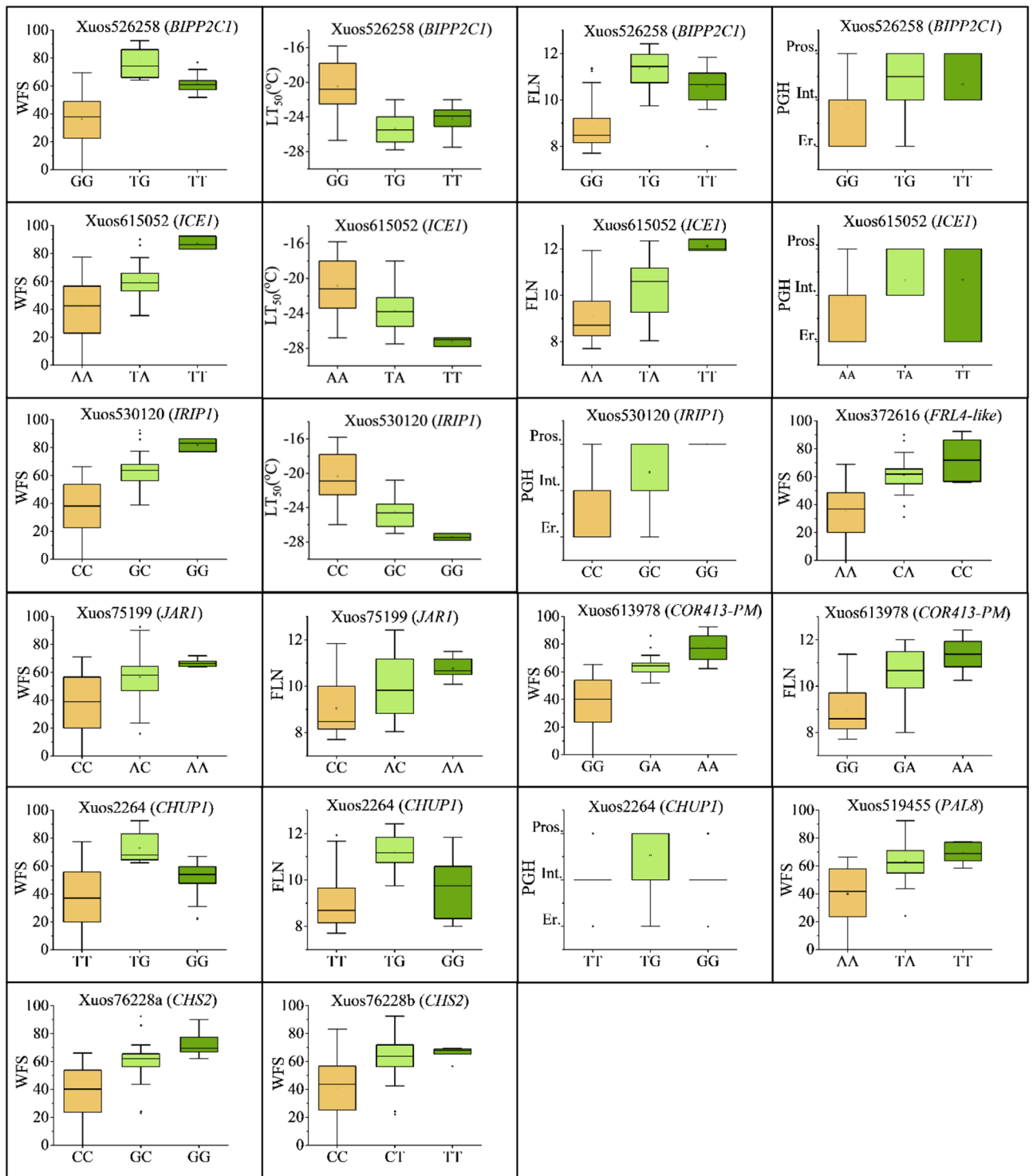


Figure 2. Box-whisker plots showing the allele effects for the most significant ($p < 1.49 \times 10^{-4}$) MTAs. The plots show median (horizontal bar), interquartile ranges (boxes), ranges (whiskers), and outliers (dots) for marker allele frequencies among the 96 rye genotypes.

ing to NetPhos 3.1 analysis. Genotypes with low or very low WFS encoded only the A₃₀ variant for COR413-PM, which was also associated with low FLN (Fig. 2; Table S4). High WFS and FLN values were associated with the T₃₀ modification for COR413-PM (Fig. 2; Table S4).

Inducer of CBF expression 1 (ICE1). Marker Xu615052 associated with WFS, LTT, FLN and PGH (Table 2) coincided with an *Inducer of CBF Expression 1 (ICE1)* gene (*SECCE3Rv1G0209310.1*) positioned on chromosome 3R (937,715 Mb; Fig. 4). Like the related ICE2, ICE1 is a MYC-like basic helix-loop-helix (bHLH)

transcription factor, which binds to *MYC*-recognition sequences present in *CBF* promoter regions and thereby stimulate cold-induced *CBF* expression^{73,74}. Induced *CBFs* then activate cold-dependent and abscisic acid-independent expression of *COR* genes conferring cold tolerance in plants³⁷. *SECCE3Rv1G0209310.1* showed 97% sequence identity to orthologous *TaICE41* on chromosomes 3D in hexaploid wheat, which contributes to increased freezing tolerance when overexpressed in *Arabidopsis*⁷⁵. The Xuos615052 SNP caused a L₂₈₃/H₂₈₃ variation at the end of the DNA-binding bHLH domain and start of a ZIP dimerization domain based on domain structures predicted for ICE proteins⁷⁶ (Fig. S4). Similar to the rye H₂₈₃ ICE1 variant, a basic residue (K) is present at corresponding site for ICE1 isoforms XI and X2 produced by *Aegilops tauschii* subsp. *tauschii* (XP_020168495 and XP_020168503), *AenICE2* of *Aegilops neglecta*, and *AeuICE2* of *Aegilops umbellulata*, respectively⁷⁷. Among 38 rye genotypes with low or very low WFS, 33 encoded only the H₂₈₃ ICE1 variant (Table S4), which was also associated with low LTT, low FLN, and erect growth habit (Fig. 2). Most (24 out of 39) rye genotypes with very high and high WFS encoded only L₂₈₃ or both variants (L₂₈₃/H₂₈₃) for ICE1 (Fig. 2; Table S4).

Jasmonate-resistant 1 (JAR1). Two markers, Xuos75199 (Table 2) and Xuos75046 (Table S3), both associated with WFS and FLN, targeted the same gene, (*SECCE1Rv1G0061510.1*) on chromosome 1R (716,318 Mb; Fig. 4). The *SECCE1Rv1G0061510.1* transcript showed strong sequence identity (95%) to an *Aegilops tauschii* subsp. *tauschii*, *Jasmonate-resistant 1 (JAR1)* mRNA isoform X3. JAR1 is a cytosolic auxin-inducible enzyme catalyzing reversible conversion of Jasmonic Acid (JA) to JA-Ile, which is the active growth regulator in JA signaling⁷⁸. Both JA and methyl jasmonate (MeJA) can be converted to JA-Ile and participate in the activation of systemic defense; thus, JA is involved in several stress responses⁷⁹. The more significant SNP for JAR1 (Xuos75199) caused an N₁₁/T₁₁ variation, of which the T₁₁ variant was common among genotypes with low or very low WFS (29 out of 38 genotypes; Table S4) and associated with low FLN values (Fig. 2). JAR1 encoded by genotypes with high and very high WFS generally carried alleles coding for both (N₁₁/T₁₁) variants (Fig. 2; Table S4).

FRIGIDA-like 4 (FRL4-like). Marker Xuos372616 associated with WFS corresponded to *SECCE5Rv1G0358510.1* located on chromosome 5R (755,939 Mb; Table 2; Fig. 4) and coding for a FRIGIDA-like protein based on BLASTp searches. High sequence identities were also noted to a C-terminal FRIGIDA-like domains carried by 5'-3' exoribonuclease 4 (XRN4) proteins encoded by *Brachypodium distachyon* (XP_024313537), *Oryza sativa* (XP_025879725), and *Triticum urartu* (EMS54431.1). Interestingly, *SECCE5Rv1G0358500.1* located 1,343 bp upstream and oriented in the same direction as *SECCE5Rv1G0358510.1* codes for a XRN4-like protein without the FRIGIDA-like domain. As evidence is lacking for a rye transcript coding for both XRN4 and FRIGIDA-like domains, we assume the gene targeted by Xuos372616 only encoded the FRIGIDA-like protein. Amino acid alignment to FRIGIDA-like proteins characterized in *Arabidopsis*⁸⁰ revealed the rye FRIGIDA-like protein had highest similarity (59–61%; data not shown) to subfamily IV represented by AtFRL4a and AtFRL4b. *AtFRL4b* is co-regulated with genes encoding chromatin remodeling factors and proteins involved in floral transition⁸¹ and maize *FRL4* also participates in a chromatin remodeling network involving MADS box factors controlling floral development⁸². However, no information regarding *FRL4* action among *Triticeae* species is available. For the rye FRL4-like protein, the Xuos372616 SNP did not alter the encoded amino acid (A₂₃₅). Homozygous A/A alleles at SNP site dominated among genotypes with low or very low WFS (36 out of 38), whereas both (C/A) alleles were frequent among genotypes with very high and high WFS (21 out of 39). (Fig. 2; Table S4). *FRL4*-like gene seems a reasonable candidate gene for Xuos372616; however, it cannot be excluded that the upstream *SECCE5Rv1G0358500.1* encoding XRN4 or a protein with both XRN4 and FRIGIDA-like domains is the actual gene causing the trait variance.

Chloroplast unusual positioning protein-1 (CHUP1). Two of the markers identified in the study coincided with genes controlling chloroplast movement. Marker Xuos2264 associated with WFS, FLN, and PGH was of higher significance (Table 2) and corresponded to *SECCE1Rv1G0013960.1* gene positioned on chromosome 1R (109,131 Mb; Fig. 4). This gene codes for a Chloroplast Unusual Positioning Protein-1 (CHUP1), but the Xuos2264 SNP variation T/G did not alter the protein sequence at G₂. Genotypes with low and very low WFS generally carried the T allele at SNP position, whereas both SNP variants were preferred by genotypes with high WFS (Table S4). The second chloroplast movement marker (Xuos370689) was only significant for WFS (Table S3) and matched *SECCE5Rv1G0331080.1* positioned on chromosome 5R (536.242 Mb; Fig. 4). The Xuos370689 marker targeted a *WEAK CHLOROPLAST MOVEMENT UNDER BLUE LIGHT 1 (WEB1)* gene, for which SNP variation (A/G) was synonymous (R₃₁₀/R₃₁₀). CHUP1, which is localized in the chloroplast envelope, regulates polymerization and/or maintenance of chloroplast actin (cp-actin), which mediates blue light-regulated translocation of chloroplasts to specific sites on the plasma membrane depending on the intensity of incoming light⁸³. WEB1 has a role in blue-light-induced reorganization of cp-actin filaments during the avoidance response and is associated with the speed chloroplast move⁸⁴. The identification of highly significant SNPs targeting two different genes involved in chloroplast relocation suggest positioning of chloroplasts could be an important factor for WFS in rye.

Phenylalanine Ammonia-lyase 8 (PAL8) and Chalcone Synthase 2 (CHS2). Among the highly significant markers for WFS were markers for genes encoding enzymes in the phenylpropanoid pathway. A Phenylalanine Ammonia-lyase 8 (PAL8) gene (*SECCE6Rv1G0399250.1*) located on chromosome 6R (434.208 Mb; Fig. 4; Table 2) was targeted by marker Xuos519455 and a Chalcone Synthase 2 (CHS2) gene (*SECCE2Rv1G0140890.1*) by two markers (Xuos76228a and Xuos76228b) on chromosome 2R (933,364 Mb; Fig. 4; Table 2). PAL is the first enzyme in the general phenylpropanoid pathway and catalyzes channeling of *L*-Phe from the primary metabo-

lism to synthesis of *trans*-cinnamic acid. This enzymatic step constitutes the starting point for numerous polyphenol compounds such as flavonols, stilbenes, lignin, and anthocyanins in plants⁸⁵. At the Xuos519455 SNP site for PAL8, a F₂₉₁/L₂₉₁ variation was encoded. The alternative L₂₉₁ variant was very common in genotypes with low and very low WFS (35 out of 38), whereas the reference F₂₉₁ allele was primarily encoded by the most winter-hardy genotypes (Fig. 2; Table S4). CHS2 acts downstream of PAL and diverts compounds away from the general phenylpropanoid pathway and towards flavonoids by catalyzing condensation of three malonyl-CoA molecules with one 4-coumaroylCoA molecule to form naringenin chalcone. The Xuos76228a SNP caused a Q₇₉/E₇₉ variation and Xuos76228b SNP an A₁₀₄/V₁₀₄ variation for CHS2 predicted from *SECCE2Rv1G0140890.1*. The reference Q₇₉ and A₁₀₄ residues were favored by genotypes with low and very low WFS (34 out of 38 genotypes; Fig. 2; Table S4), whereas the alternative E₇₉ and V₁₀₄ residues were most common among genotypes with very high WFS (Fig. 2; Table S4).

Variation for CBF genes showed low significance for WFS. In this study, three markers significant for WFS matched CBF genes at *FR-R2* on chromosome 5R, but at lower significance level ($p < 0.01$; Table S3) than those listed in Table 2. The genes targeted by markers Xuos369733, Xuos390086, and Xuos370362 were *CBFIIIa-19* (*SECCE5Rv1G0340540.1*), *CBFIVa-2.2* (*SECCE5Rv1G0340460.1*), and *CBFIIIa-6.2* (*SECCE5Rv1G0340660.1*), respectively (5R:614.963–616.449 Mb; Fig. 4). SNP variations for *CBFIIIa-19* were synonymous (D₄₀₁/D₄₀₁), whereas SNP variation for *CBFIVa-2.2* caused an H₁₁₃/P₁₁₃ change within encoded AP2 DNA-binding region and immediately prior to signature motif CMIII-1 (Fig. S4). SNP variation for *CBFIIIa-6.2* resulted in a L₂₂₄ to H₂₂₄ variation within CBFIIIa-6.2 C-terminal region (Fig. S4). A preference for the alternative alleles for *CBFIVa-2.2* (P₁₁₃), and *CBFIIIa-6* (H₂₂₄) was found for genotypes with low or very low WFS (data not shown). Besides CBFs at *FR-A2*, Xuos328096 marker associated with FLN matched *SECCE4Rv1G0278790.1* encoding CBFII-5 from chromosome 4R (810.923 Mb; Fig. 4). The SNP at *CBFII-5* caused an R₃₇ to P₃₇ change within conserved signature sequence CMIII-3 (Fig. S4), which is essential for *Arabidopsis* CBF1 transcriptional activity⁸⁶. Whether any of the amino acid variations identified for CBFIVa-2.2, CBFIIIa-6, or CBFII-5 affected CBF function in rye remains to be demonstrated.

Bi-plot analysis supports WFS and associated traits are controlled by several common factors. The four traits analyzed in the study were analyzed by PCA, which revealed relatively high amount of trait variation explained by PC1 (50.9 to 57.8%) and PC2 (9.7 to 11.3%) in the four trait bi-plots (Fig. 3). In all bi-plots, genotypes with very high and high WFS were mostly found in the first and fourth quadrants, whereas genotypes with low WFS were located in the second and third quadrants. Seven vectors representing SNP markers for candidate genes *IRIPI*, *COR413-PM*, *FRLA*-like, *JAR1*, *ICE1*, *BIPP2C1*, and *CHUP1* were visualized for each of the LTT, FLN, and PGH bi-plots, which all showed similar patterns (Fig. 3). In these three bi-plots, the first six vectors correlated relatively well with each other and contributed mainly to PC1, whereas *CHUP1* vector showed a different direction and was mainly associated with PC2. The WFS bi-plot was also represented by *IRIPI*, *COR413-PM*, *FRLA*-like, *ICE1*, and *JAR1* vectors, but in contrast to the other bi-plots, the *JAR1* vector was oriented closer to the *CHUP1* vector. WFS was also represented by two additional vectors (markers Xuos527421, Xuos615123; Table S3) corresponding to gibberellin 2-beta-dioxygenase D11 (*GA2OX-D11*; 7R:105.61 Mb) and expansin-like A1 (*EXLA1*; 5R:823.29 Mb) genes, respectively (Fig. 4). Both WFS and PGH were associated with *GA2OX-D11* (Xuos527421_WFS; Xuos527421_PGH; Table S3), which encodes an enzyme deactivating gibberellins and stimulating of compact growth⁸⁷, which is generally displayed by winter-hardy cereals. Expansins have a role in cell wall loosening causing changes to cell wall elasticity and are generally associated with stress responses affecting plant growth; however, the exact function for *EXLA1* is not known⁸⁸.

Discussion

Rye, a model for study of winter hardiness in cereals. The LD decay rate is the major factor limiting mapping resolution in GWAS and it is largely determined by the mating system (self or out-crossing), recombination rate, distribution of recombination hot spots on the genome, and population structure⁸⁹. In this respect, rye with a low average intra-genic LD of about 4.3 kb (Table S2) or less⁵ is well suited for association mapping, which provides a considerable higher mapping resolution than bi-parental mapping⁴¹. In this study, the mapping precision was further improved by using a reduced-representation GBS library targeting low-copy hypomethylated regions for SNP identification⁴⁴. Successful accomplishment of this strategy was demonstrated by 90 out of 189 (47.6%) significant SNP markers mapped to annotated genes (Table S3).

The PCA and STRUCTURE analyses grouped the rye population of 96 genotypes into three main subpopulations (Figs. 1, S1, S2; Table S1). Many of the winter-hardy Canadian rye cultivars were grouped together with genotypes with relatively low winter-hardiness levels (Table S1). Overall, the clustering of rye genotypes did not relate well to their geographical origin or WFS values (Table S1), but a slight preference around the Carsten genepool was indicated for genotypes with very high WFS (Fig. 1; Table S1). Although breeding has reduced the genetic pool of rye⁶, it has still been possible to select/develop very cold hardy rye varieties with winter hardiness far exceeding that of wheat and barley cultivars, which have undergone loss of diversity for genes conferring high WFS. Thus, the key genetic factors required to improve winter hardiness in tender winter cereals are present in certain rye genotypes.

Adjustment of photosynthesis during cold acclimation. Allele differences for *CHUP1* and *WEB1* encoding proteins involved in chloroplast movement^{83,84,90} were associated with WFS levels within the rye population (Table S3). *CHUP1* allele variation was also suggested by the PCA bi-plot analysis to affect PGH, FLN, and LTT trait values (Fig. 3), which are determined during the cold acclimation process. Chloroplast movement to

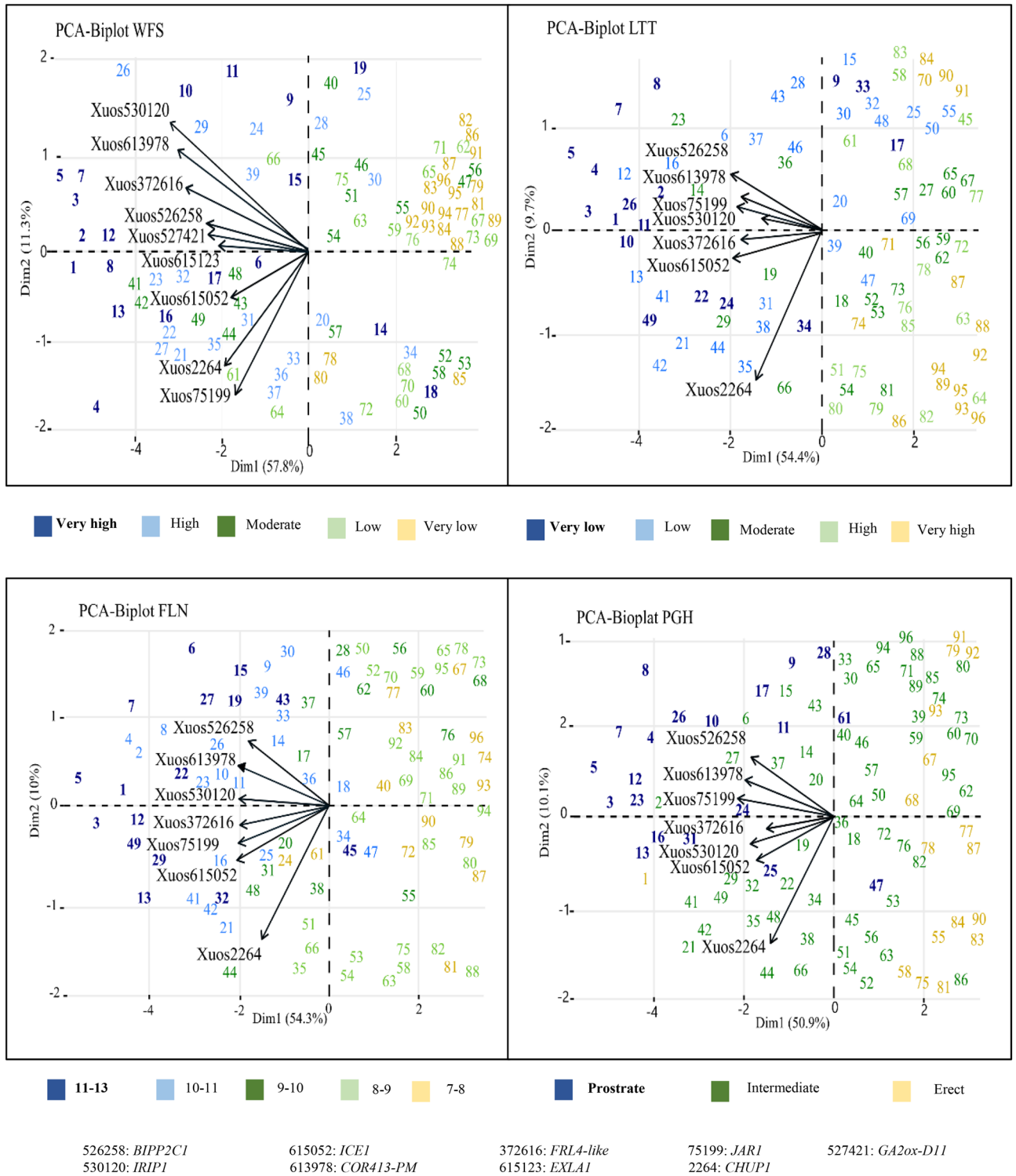


Figure 3. PCA bi-plot visualizing SNP effects on four traits analyzed for rye population of 96 genotypes.

the periclinal cell wall is suggested to enhance photosynthesis and biomass production under low light conditions, whereas movement to anticlinal cell wall was initially postulated to protect the photosynthetic apparatus from high light⁹¹. Later studies suggest the avoidance reaction fine-tunes light signals or regulates signaling pathways⁹⁰. Chloroplasts have a very important role during cold acclimation in winter cereals, as they adjust the photosynthesis efficiency upon response to environmental temperature and light signals^{11,92}. This allows certain cold-hardy winter cereals to increase their photosynthesis efficiency during cold acclimation when compared to less winter-hardy genotypes²¹. A study in *Arabidopsis* supports the photosynthetic acclimation depends on chloroplast relocation which coordinates photosynthesis with down-stream carbohydrate metabolism⁹³. Retrograde and anterograde signaling during cold stress may also be affected by chloroplast repositioning as nuclei attach

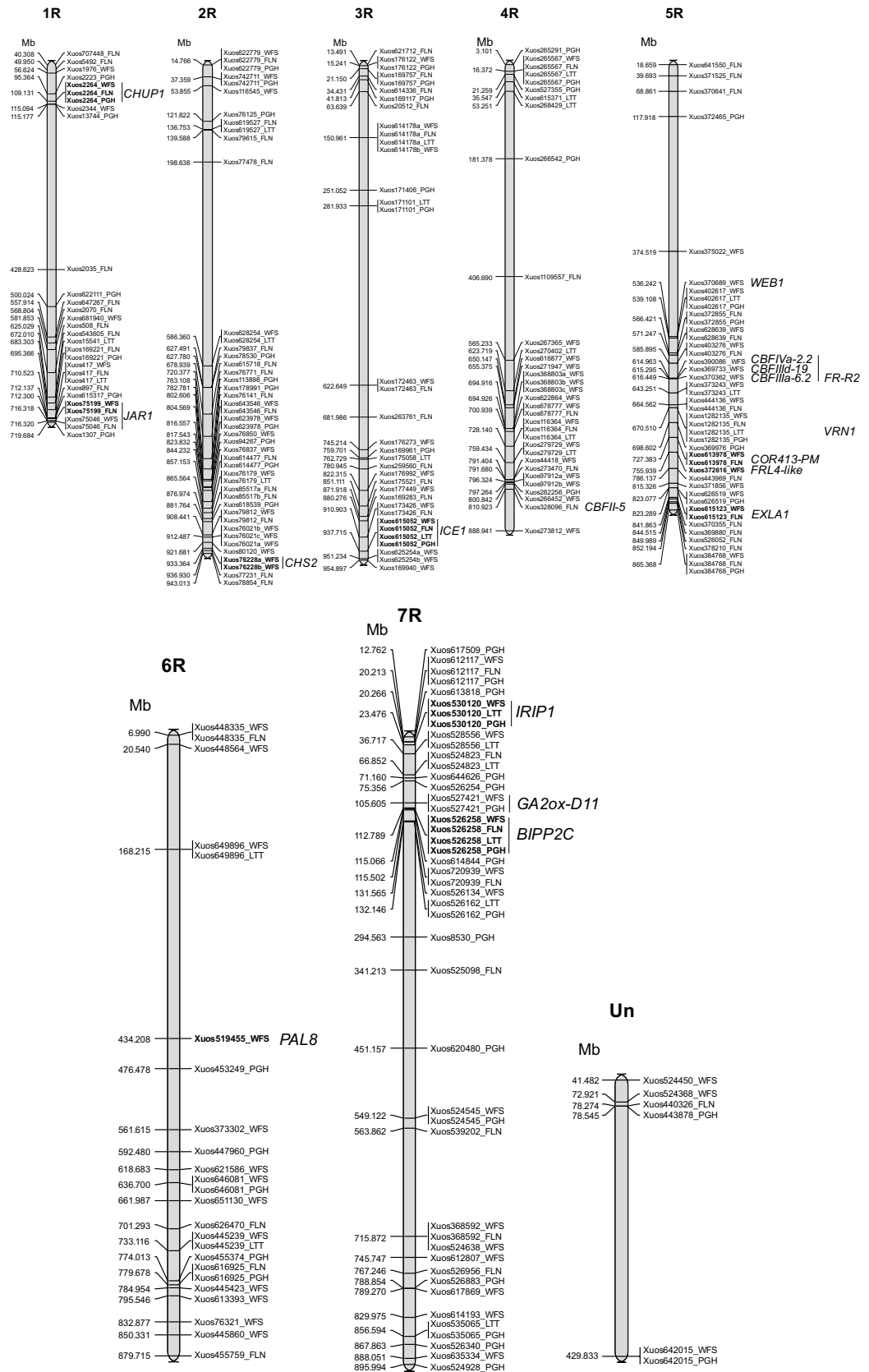


Figure 4. Location of significant MTAs identified on rye physical map. Locations refers to the Lo7 v1 pseudomolecules 2021⁴. Most significant markers ($p < 1.49e-04$; Table 2) are indicated in bold. Location of *FR-R2*, *VRN1*, and discussed candidate genes are shown.

and co-migrate with chloroplasts to new destinations on the plasma membrane⁹⁴. Although no amino acid difference was associated with SNP variations for *CHUP1* or *WEB1*, it is possible these genes are differentially regulated by light and/or temperature signals in rye genotypes with varying degree of WFS. Further analysis of rye *CHUP1* and *WEB1* genes and expression levels during cold acclimation are needed to confirm their role during cold acclimation in rye.

Protection of membrane integrity during cold acclimation. Like the organelle membranes, the plasma membrane is prone to freezing injury and must be protected to withstand cell dehydration caused by apoplastic freezing and membrane fracturing by growing ice crystals. The protection mechanisms generally include membrane rigidification⁹⁵, production of proteins with membrane stabilization properties⁹⁶, and prevention of ice crystal formation and growth⁹⁷. One of the cold-induced plasma membrane proteins is the multi-spanning *COR413-PM*, for which sequence variation was associated with WFS and FLN (Table 2). Overexpression of *PsCOR413PM2* isolated from *Phlox subulata* in *Arabidopsis* causes an increased Ca^{2+} flux in roots and higher expression of *CBF1*, *CBF3* and certain *COR* genes not induced by CBFs⁹⁸. Thus, *COR413* acts early in the cold-induction pathway and both *COR413-PM1* and related chloroplast *COR413-IM* in *Arabidopsis* are included in a set of 56 plant core environmental stress genes triggering systemic stress responses; however, the systemic signal inducing this response is not known⁹⁹. Although the precise *COR413-PM* function has not been determined, it has been suggested the membrane-bound protein maintains membrane fluidity at low temperature¹⁰⁰, acts as a G protein-coupled receptor involved in signaling⁷², or stabilizes the membrane lipid structure⁹⁸.

Like *COR413-PM*, IRIPs are important for membrane protection. In this study, WFS, LTT, and PGH for the rye population were strongly associated with allelic variation for one of many IRIP genes encoded from a 7R locus (Table 2). IRIPs contribution to frost-hardiness is supported by an increased *IRIP* expression during cold acclimation in wheat¹⁰¹ and improved freezing tolerance in transgenic *Arabidopsis* expressing *LpIRI-a*, *LpIRI-b*, *LpIRI2*, or *LpIRI3* from *Lolium perenne*¹⁰². A reduced freezing tolerance caused by down-regulation of *IRIPs* in *Brachypodium distachyon* further confirms ice-binding proteins contribute to development of frost tolerance in cereals⁶⁹. Prevention of ice crystal growth in the apoplast is particularly critical during freeze/thaw cycles, which may occur during winter or early spring for winter cereals.

Unexpectedly, our study suggested IRIP sequence variation affected PGH (Table 2), which is caused by curvature of shoots emerging from the crown during cold acclimation. The phenotype is likely due to altered gravitropic responses affecting auxin distribution at the shoot base¹⁰³. The shoot is one of first plant tissues that freezes, despite the lower part of the plant is warmer than the upper part⁶⁸. Thus, very cold hardy cereals have evolved a more efficient frost protection for SAM than less cold-hardy genotypes to assure survival of the crown during winter and regrowth in the spring. The association between *IRIP1* variation and PGH suggests the ice-binding proteins are produced at SAM; however, there is no information regarding expression levels of *IRIP* genes in rye crowns. In wheat, JA and ethylene activate *TaIRIP-1* expression in leaves, crowns, and roots during cold acclimation, but the two phytohormones do not activate *TaIRIP-2*, which is only expressed in leaves⁶⁷. Thus, studies of tissue-specific expression of *IRIP* alleles are needed to reveal which *IRIP* isoform(s) encoded from 7R affects PGH and possibly SAM development during cold acclimation.

Candidate genes belonging to the ICE-CBF-COR regulon. Like other *Triticeae* members, rye *Fr-R2* carries a cluster of *CBF* genes¹⁰⁴, for which haplotype variation is suggested to underlie differences in freezing tolerance among rye accessions^{4,36}. However, the significant associations between WFS and three different *CBF* genes (*CBFIIIa-D19*, *CBFIVa-2.2*, and *CBFIIIa-6*) at *FR-R2* were not among the strongest MTAs (Table S3). Transcript analysis of rye *CBF* genes indicates existence of three *CBFIVa-2.2* and two *CBFIIIa-6* genes¹⁰⁵. This could possibly explain the low significance for individual *CBF* alleles as complementary functions may be exerted by additional copies of near-identical *CBF*; thus, SNP variations for multi-copy *CBF* genes contribute little to phenotype differences within the population. Lack of strong association between SNP variations for individual *CBF* genes at *Fr-A2* and frost resistance is also seen in a panel of 1739 European winter wheat genotypes studied by association mapping¹⁰⁶. However, most mapping studies of bi-parental populations in wheat, barley, and rye show *Fr-2* has a major role for frost tolerance^{35,107,108}. Due to the limited number of recombination events and narrow genetic variation within the populations studied, the bi-parental confidence intervals for QTL regions are large, and for the *FR* loci on group five chromosomes, defined by a composite effect from several *CBF* genes, their expression levels, interactions, and copy number effects.

Although variation for individual *CBF* genes appeared to have a minor role for WFS, several candidate genes belonging to the ICE-CBF-COR regulon were identified. One strong candidate gene was *ICE1* (Table 2), for which amino acid variation at the end of the DNA binding bHLH region and/or start of zipper region was associated with WFS, LTT, FLN and PGH (Fig. S4). In a previous study, allele variation within an intron for *ScICE2*, probably allelic with *ICE1* identified in this study, was associated with variation for winter hardiness and freezing tolerance among 201 European rye genotypes³⁶. Thus, specific *ICE* alleles may be important for winter hardiness in rye. Since genotypes with low or very low WFS generally encoded *ICE1* containing the rare H₂₈₃ modification, these *ICE1* proteins may display reduced affinity for the MYC recognition elements (CANNTG) present in promoters of *CBF* genes and several other cold-regulated genes^{73,74}. Alternatively, the H₂₈₃ *ICE1* variation, which is also located at the start of the ZIP domain, could affect dimer formation⁷⁶. Through heterodimers formed with various bHLH factors, both *ICE1* and *ICE2* have a role in the establishment and differentiation of stomata in dicot plants¹⁰⁹ and stomata lineage formation in monocot plants¹¹⁰. Through similar heterodimer formations, additional developmental roles for rye *ICE1* may exist at SAM as *ICE1* allele variation in this study was associated with both FLN and PGH besides WFS and LTT (Table 2).

Study suggests jasmonic acid influences cold acclimation and floral transition. Allele variations for *JAR1* was associated with WFS and FLN in our study (Table S3). In support of *JAR1* causing variation for WFS in rye are previous studies demonstrating JA has a role in the development of cold stress resistance in *Arabidopsis*^{26,111}. These studies show cold-induced JA-Ile production leads to activation of the *ICE-CBF-COR* regulon, which could explain the association between *JAR1* and WFS observed in our study (Table 2). The association between *JAR1* and FLN (Table 2) further suggested JA-Ile influences timing of vegetative to reproductive transition at SAM during cold acclimation. Such a role for *JAR1* is supported by studies in maize and rice associating *JAR1* activity with delayed juvenile-to-adult transition at SAM in both species^{112,113}. During vernalization in wheat, the MeJA levels are shown to increase, but they decline post-vernalization when plants return to normal temperature¹¹⁴. An increased expression of *VRN1* and *VRN3* and delayed flowering is demonstrated by exogenous application of MeJA to spring wheat, which suggests JA regulates vernalization requirement and modulates flowering time in wheat¹¹⁴. Thus, it is possible the association between *JAR1*, WFS and FLN observed in our study involves *JAR1*-mediated regulation of *VRN1* with effects on timing of floral transition.

Another JA-induced effect during cold acclimation in *Arabidopsis* is biosynthesis of cold-protective secondary metabolites, such as polyamines, glutathione, and anthocyanins^{26,115}. The production of glycosylated cyanins in particular is associated with enhanced winter hardiness in rye population analyzed in this study¹¹⁶. Thus, allele variations for *JAR1* and two of the genes encoding early enzymes in the phenylpropanoid pathway, *PAL8*, *CHS2* (Table 2), may have a role in increasing anthocyanin levels during cold acclimation in several of the most winter-hardy genotypes. JA can also affect cold acclimation independent of the CBF pathway whereby growth is regulated¹¹⁷. Thus, *JAR1* can have many different roles during and after cold acclimation, which may be reflected in the different positions of the *JAR1* vector in the WFS bi-plot versus the LTT, FLN, PGH bi-plots (Fig. 3).

Expansion of stress related alleles in winter-hardy rye. Rye genotypes with high and very high WFS showed an overall higher frequency of allele variants for candidate genes than genotypes with low or very low cold hardiness (Fig. 3; Table S4). This tendency was particularly obvious for *IRIP1*, *COR413-PM*, *FRL4-like*, *BIPP2C1*, *CHUP1*, *CHS2* and *PAL8*. The trend suggested the most winter-hardy genotypes have evolved higher fitness to winter conditions through acquisition of additional alleles for some of the important cold-responsive genes. A wide-spread duplications of rye genes as compared to other cereals is supported by a recent near full-length (98.47%) genome assembly of Chinese rye line Weining with a low heterozygosity rate of 0.26%¹¹⁸. Similar to the expansion of *CBF* and *IRIP* gene families that occurred when Pooideae lineages adapted to extreme temperatures during the Eocene–Oligocene transition^{68,119}, the extra alleles for some of the cold-regulated candidate genes identified in this study may have evolved during periods of cold stress in the history of rye. Gene expansion is not unique to cereals, but has occurred throughout the evolutionary history of plants and is predominantly observed for stress-responsive genes¹²⁰. Whether the additional gene copy number for cold-responsive genes identified by our study provides that extra winter-hardiness observed for some of the Canadian rye cultivars when compared to other rye genotypes needs to be explored further.

Concluding remarks

The phenotypic relationships reported earlier for the rye population studied here showed that sub-traits like LTT, FLN, and PGH with high heritability estimates ($h^2 = 0.45$ to 0.81), can be used to dissect a complex trait like WFS⁴⁰. With the abundance of SNP markers provided by GBS combined with a draft genome sequence for rye, the association mapping conducted on the rye population identified in total 90 annotated candidate genes ($p < 0.01$). The accuracy of the mapping is strengthened by finding seven of the nine strongest candidate genes have roles in plant adaptation during cold acclimation and contribute to enhanced winter hardiness in cereals and other plants. For two strong candidate genes, *BIPP2C* and *FRL4-like*, there are no obvious associations to WFS in *Triticeae* species. As similar genes in other monocot species are implicated in floral transition, studies of the rye *BIPP2C* and *FRL4-like* is likely to advance our knowledge of the cold tolerance process in winter cereals. Thus, future studies are planned with a diverse panel of rye genotypes with varying LTT and/or WFS to validate all the candidate genes identified in this study, many of which seem promising but were not discussed here. The long-term objective is to verify gene variants that enhance winter hardiness in rye and use this information to increase WFS in temperate winter cereals of interest for the Northern hemisphere. Identification of genetic factors contributing to WFS in winter cereals is of particular importance considering the immediate challenges of global warming increasing the demand for crops with higher resilience to variable weather patterns.

Data availability

All data used in the study is included in the manuscript and in the supplementary data files.

Received: 20 September 2021; Accepted: 25 March 2022

Published online: 06 April 2022

References

- Schlegel, R. H. J. *RYE. Genetics, Breeding, and Cultivation* (CRC Press, Boca Raton, 2014).
- Martis, M. M. *et al.* Reticulate evolution of the rye genome. *Plant Cell* **25**, 3685–3698 (2013).
- Bauer, E. *et al.* Towards a whole-genome sequence for rye (*Secale cereale* L.). *Plant J.* **89**, 853–869 (2017).
- Rabanus-Wallace, M. T. *et al.* Chromosome-scale genome assembly provides insights into rye biology, evolution and agronomic potential. *Nat. Genet.* **53**, 564–573 (2021).
- Li, Y. *et al.* High levels of nucleotide diversity and fast decline of linkage disequilibrium in rye (*Secale cereale* L.) genes involved in frost response. *BMC Plant Biol.* **11**, 6 (2011).

6. Targońska, M., Bolibok-Bragoszewska, H. & Rakoczy-Trojanowska, M. Assessment of genetic diversity in *Secale cereale* based on SSR markers. *Plant Mol. Biol. Rep.* **34**, 37–51 (2016).
7. Fowler, D. B., Byrns, B. M. & Greer, K. J. Overwinter low-temperature responses of cereals: Analyses and simulation. *Crop Sci.* **54**, 2395–2405 (2014).
8. Thomashow, M. F. Plant cold acclimation: Freezing tolerance genes and regulatory mechanisms. *Annu. Rev. Plant Physiol. Plant Mol. Biol.* **50**, 571–599 (1999).
9. Trevasakis, B., Hemming, M. N., Dennis, E. S. & Peacock, W. J. The molecular basis of vernalization-induced flowering in cereals. *Trends Plant Sci.* **12**, 352–357 (2007).
10. Franklin, K. A. & Whitelam, G. C. Light-quality regulation of freezing tolerance in *Arabidopsis thaliana*. *Nat. Genet.* **39**, 1410–1413 (2007).
11. Kurepin, L. V. *et al.* Role of CBFs as integrators of chloroplast redox, phytochrome and plant hormone signaling during cold acclimation. *Int. J. Mol. Sci.* **14**, 12729–12763 (2013).
12. Fowler, D. B. & Limin, A. E. Interactions among factors regulating phenological development and acclimation rate determine low-temperature tolerance in wheat. *Ann. Bot.* **94**, 717–724 (2004).
13. Livingston III, D. P. The second phase of cold hardening: Freezing tolerance and fructan isomer changes in winter cereal crowns. *Crop Sci.* **36**, 1568–1573 (1996).
14. Le, M. Q., Pagter, M. & Hinch, D. K. Global changes in gene expression, assayed by microarray hybridization and quantitative RT-PCR, during acclimation of three *Arabidopsis thaliana* accessions to sub-zero temperatures after cold acclimation. *Plant Mol. Biol.* **87**, 1–15 (2015).
15. Hüner, N. P. A., Dahal, K., Bode, R., Kurepin, L. V. & Ivanov, A. G. Photosynthetic acclimation, vernalization, crop productivity and 'the grand design of photosynthesis'. *J. Plant Physiol.* **203**, 29–43 (2016).
16. Limin, A. E. & Fowler, D. B. Morphological and cytological characters associated with low-temperature tolerance in wheat (*Triticum aestivum* L. em Thell.). *Can. J. Plant Sci.* **80**, 687–692 (2000).
17. Willick, I. R., Takahashi, D., Fowler, D. B., Uemura, M. & Tanino, K. K. Tissue-specific changes in apoplastic proteins and cell wall structure during cold acclimation of winter wheat crowns. *J. Exp. Bot.* **69**, 1221–1234 (2018).
18. Bohn, M., Lüthje, S., Sperling, P., Heinz, E. & Dörffling, K. Plasma membrane lipid alterations induced by cold acclimation and abscisic acid treatment of winter wheat seedlings differing in frost resistance. *J. Plant Physiol.* **164**, 146–156 (2007).
19. Griffith, M. & Yaish, M. W. F. Antifreeze proteins in overwintering plants: A tale of two activities. *Trends Plant Sci.* **9**, 399–405 (2004).
20. Guy, C., Kaplan, F., Kopka, J., Selbig, J. & Hinch, D. K. Metabolomics of temperature stress. *Physiol. Plant.* **132**, 220–235 (2008).
21. Dahal, K. *et al.* The effects of phenotypic plasticity on photosynthetic performance in winter rye, winter wheat and *Brassica napus*. *Physiol. Plant.* **144**, 169–188 (2012).
22. Oliver, S. N., Finnegan, E. J., Dennis, E. S., Peacock, W. J. & Trevasakis, B. Vernalization-induced flowering in cereals is associated with changes in histone methylation at the *VERNALIZATION1* gene. *Proc. Natl. Acad. Sci. U.S.A.* **106**, 8386–8391 (2009).
23. Luo, X. & He, Y. Experiencing winter for spring flowering: A molecular epigenetic perspective on vernalization. *J. Integr. Plant Biol.* **62**, 104–117 (2020).
24. Smékalová, V., Doskočilová, A., Komis, G. & Šamaj, J. Crosstalk between secondary messengers, hormones and MAPK modules during abiotic stress signalling in plants. *Biotechnol. Adv.* **32**, 2–11 (2014).
25. Eremina, M., Rozhon, W. & Poppenberger, B. Hormonal control of cold stress responses in plants. *Cell. Mol. Life Sci.* **73**, 797–810 (2016).
26. Hu, Y. *et al.* Jasmonate regulates leaf senescence and tolerance to cold stress: Crosstalk with other phytohormones. *J. Exp. Bot.* **68**, 1361–1369 (2017).
27. Crosatti, C., Rizza, F., Badeck, F. W., Mazzucotelli, E. & Cattivelli, L. Harden the chloroplast to protect the plant. *Physiol. Plant.* **147**, 55–63 (2013).
28. Cattivelli, L. *et al.* Chromosome regions and stress-related sequences involved in resistance to abiotic stress in *Triticeae*. *Plant Mol. Biol.* **48**, 649–665 (2002).
29. Zhu, J. *et al.* Copy number and haplotype variation at the *VRN-A1* and central *FR-A2* loci are associated with frost tolerance in hexaploid wheat. *Theor. Appl. Genet.* **127**, 1183–1197 (2014).
30. Bága, M., Fowler, D. B. & Chibbar, R. N. Identification of genomic regions determining the phenological development leading to floral transition in wheat (*Triticum aestivum* L.). *J. Exp. Bot.* **60**, 3575–3585 (2009).
31. Dhillon, T. *et al.* Regulation of freezing tolerance and flowering in temperate cereals: The *VRN-1* connection. *Plant Physiol.* **153**, 1846–1858 (2010).
32. Pearce, S. *et al.* Large deletions in the *CBF* gene cluster at the *Fr-B2* locus are associated with reduced frost tolerance in wheat. *Theor. Appl. Genet.* **126**, 2683–2697 (2013).
33. Würschum, T., Longin, C. F. H., Hahn, V., Tucker, M. R. & Leiser, W. L. Copy number variations of *CBF* genes at the *Fr-A2* locus are essential components of winter hardiness in wheat. *Plant J.* **89**, 764–773 (2017).
34. Francia, E. *et al.* Fine mapping of a *HvCBF* gene cluster at the frost resistance locus *Fr-H2* in barley. *Theor. Appl. Genet.* **115**, 1083–1091 (2007).
35. Erath, W. *et al.* Exploring new alleles for frost tolerance in winter rye. *Theor. Appl. Genet.* **130**, 2151–2164 (2017).
36. Li, Y. *et al.* Association analysis of frost tolerance in rye using candidate genes and phenotypic data from controlled, semi-controlled, and field phenotyping platforms. *BMC Plant Biol.* **11**, 146 (2011).
37. Stockinger, E. J., Gilmour, S. J. & Thomashow, M. F. *Arabidopsis thaliana* *CBF1* encodes an AP2 domain-containing transcriptional activator that binds to the C-repeat/DRE, a cis-acting DNA regulatory element that stimulates transcription in response to low temperature and water deficit. *Proc. Natl. Acad. Sci. U.S.A.* **94**, 1035–1040 (1997).
38. Fowler, S. & Thomashow, M. F. *Arabidopsis* transcriptome profiling indicates that multiple regulatory pathways are activated during cold acclimation in addition to the *CBF* cold response pathway. *Plant Cell* **14**, 1675–1690 (2002).
39. Jia, Y. *et al.* The *cbfs* triple mutants reveal the essential functions of *CBFs* in cold acclimation and allow the definition of *CBF* regulons in *Arabidopsis*. *New Phytol.* **212**, 345–353 (2016).
40. Bahrani, H. *et al.* The relationships between plant developmental traits and winter field survival in rye (*Secale cereale* L.). *Plants* **10**, 1–17 (2021).
41. Alqudah, A. M., Sallam, A., Baenziger, P. S. & Börner, A. GWAS: Fast-forwarding gene identification and characterization in temperate cereals: Lessons from barley—a review. *J. Adv. Res.* **22**, 119–135 (2020).
42. Nguyen, K. L., Grondin, A., Courtois, B. & Gantet, P. Next-generation sequencing accelerates crop gene discovery. *Trends Plant Sci.* **24**, 263–274 (2019).
43. Piepho, H. P., Möhring, J., Melchinger, A. E. & Büchse, A. BLUP for phenotypic selection in plant breeding and variety testing. *Euphytica* **161**, 209–228 (2008).
44. Poland, J. A., Brown, P. J., Sorrells, M. E. & Jannink, J.-L. Development of high-density genetic maps for barley and wheat using a novel two-enzyme genotyping-by-sequencing approach. *PLoS ONE* **7**, 32253 (2012).
45. Mascher, M., Wu, S., St. Amand, P., Stein, N. & Poland, J. Application of genotyping-by-sequencing on semiconductor sequencing platforms: A comparison of genetic and reference-based marker ordering in barley. *PLoS One* **8**, 76925 (2013).

46. Bolger, A. M., Lohse, M. & Usadel, B. Trimmomatic: A flexible trimmer for Illumina sequence data. *Bioinformatics* **30**, 2114–2120 (2014).
47. Langmead, B. & Salzberg, S. L. Fast gapped-read alignment with Bowtie 2. *Nat. Methods* **9**, 357–359 (2012).
48. Li, H. A statistical framework for SNP calling, mutation discovery, association mapping and population genetical parameter estimation from sequencing data. *Bioinformatics* **27**, 2987–2993 (2011).
49. Danecek, P. *et al.* The variant call format and VCFtools. *Bioinformatics* **27**, 2156–2158 (2011).
50. Bradbury, P. J. *et al.* TASSEL: Software for association mapping of complex traits in diverse samples. *Bioinformatics* **23**, 2633–2635 (2007).
51. Myers, T. A., Chanock, S. J. & Machiela, M. J. LDlinkR: An R package for rapidly calculating linkage disequilibrium statistics in diverse populations. *Front. Genet.* **11**, 1–5 (2020).
52. Pritchard, J. K., Stephens, M. & Donnelly, P. Inference of population structure using multilocus genotype data. *Genetics* **155**, 945–959 (2000).
53. Earl, D. A. & VonHoldt, B. M. STRUCTURE HARVESTER: A website and program for visualizing STRUCTURE output and implementing the Evanno method. *Conserv. Genet. Resour.* **4**, 359–361 (2012).
54. Evanno, G., Regnaut, S. & Goudet, J. Detecting the number of clusters of individuals using the software STRUCTURE: A simulation study. *Mol. Ecol.* **14**, 2611–2620 (2005).
55. Chavent, M., Kuentz-Simonet, V. & Saracco, J. Orthogonal rotation in PCAMIX. *Adv. Data Anal. Classif.* **6**, 131–146 (2012).
56. Nei, M. Genetic distance between populations. *Am. Nat.* **106**, 283–292 (1972).
57. Benjamini, Y. & Hochberg, Y. Controlling the false discovery rate: A practical and powerful approach to multiple testing. *J. R. Stat. Soc. B* **57**, 289–300 (1995).
58. Robertson, D. S., Wildenhain, J., Javanmard, A. & Karp, N. A. OnlineFDR: An R package to control the false discovery rate for growing data repositories. *Bioinformatics* **35**, 4196–4199 (2019).
59. International Wheat Genome Sequencing Consortium (IWGSC). Shifting the limits in wheat research and breeding using a fully annotated reference genome. *Science* **361**, eaar7191 (2018).
60. Voorrips, R. E. Mapchart: Software for the graphical presentation of linkage maps and QTLs. *J. Hered.* **93**, 77–78 (2002).
61. Fischer, S. *et al.* Molecular marker assisted broadening of the Central European heterotic groups in rye with Eastern European germplasm. *Theor. Appl. Genet.* **120**, 291–299 (2010).
62. Xue, T. *et al.* Genome-wide and expression analysis of protein phosphatase 2C in rice and Arabidopsis. *BMC Genomics* **9**, 550 (2008).
63. Singh, A., Giri, J., Kapoor, S., Tyagi, A. K. & Pandey, G. K. Protein phosphatase complement in rice: Genome-wide identification and transcriptional analysis under abiotic stress conditions and reproductive development. *BMC Genomics* **11**, 435 (2010).
64. Yu, X. *et al.* Genome-wide identification and homoeologous expression analysis of PP2C genes in wheat (*Triticum aestivum* L.). *Front. Genet.* **10**, 561 (2019).
65. Hu, X., Song, F. & Zheng, Z. Molecular characterization and expression analysis of a rice protein phosphatase 2C gene, *OsBI-PP2C1*, and overexpression in transgenic tobacco conferred enhanced disease resistance and abiotic tolerance. *Physiol. Plant.* **127**, 225–236 (2006).
66. Ni, L. *et al.* Abscisic acid inhibits rice protein phosphatase PP45 via H₂O₂ and relieves repression of the Ca²⁺/CaM-dependent protein kinase DMI3. *Plant Cell* **31**, 128–152 (2019).
67. Tremblay, K., Ouellet, F., Fournier, J., Danyluk, J. & Sarhan, F. Molecular characterization and origin of novel bipartite cold-regulated ice recrystallization inhibition proteins from cereals. *Plant Cell Physiol.* **46**, 884–891 (2005).
68. Sandve, S. R., Rudi, H., Asp, T. & Rognli, O. A. Tracking the evolution of a cold stress associated gene family in cold tolerant grasses. *BMC Evol. Biol.* **8**, 245 (2008).
69. Bredow, M., Vanderbeld, B. & Walker, V. K. Knockdown of ice-binding proteins in *Brachypodium distachyon* demonstrates their role in freeze protection. *PLoS One* **11**, 016794 (2016).
70. Tomalty, H. E. & Walker, V. K. Perturbation of bacterial ice nucleation activity by a grass antifreeze protein. *Biochem. Biophys. Res. Commun.* **452**, 636–641 (2014).
71. Colton-Gagnon, K. *et al.* Comparative analysis of the cold acclimation and freezing tolerance capacities of seven diploid *Brachypodium distachyon* accessions. *Ann. Bot.* **113**, 681–693 (2014).
72. Breton, G., Danyluk, J., Frenette Charron, J.-B. & Sarhan, F. Expression profiling and bioinformatic analyses of a novel stress-regulated multispansing transmembrane protein family from cereals and Arabidopsis. *Plant Physiol.* **132**, 64–74 (2003).
73. Chinnusamy, V. *et al.* ICE1: a regulator of cold-induced transcriptome and freezing tolerance in Arabidopsis. *Genes Dev.* **17**, 1043–1054 (2003).
74. Tang, K. *et al.* The transcription factor ICE1 functions in cold stress response by binding to the promoters of CBF and COR genes. *J. Integr. Plant Biol.* **62**, 258–263 (2020).
75. Badawi, M. *et al.* Structure and functional analysis of wheat ICE (inducer of CBF expression) genes. *Plant Cell Physiol.* **49**, 1237–1249 (2008).
76. Xu, W. *et al.* Chinese wild-growing *Vitis amurensis* ICE1 and ICE2 encode MYC-type bHLH transcription activators that regulate cold tolerance in Arabidopsis. *PLoS One* **9**, 102303 (2014).
77. Jin, Y. *et al.* Identification of genes from the ICE–CBF–COR pathway under cold stress in *Aegilops-Triticum* composite group and the evolution analysis with those from *Triticeae*. *Physiol. Mol. Biol. Plants* **24**, 211–229 (2018).
78. Fonseca, S. *et al.* (+)-7-iso-Jasmonoyl-L-isoleucine is the endogenous bioactive jasmonate. *Nat. Chem. Biol.* **5**, 344–350 (2009).
79. Wasternack, C. & Song, S. Jasmonates: Biosynthesis, metabolism, and signaling by proteins activating and repressing transcription. *J. Exp. Bot.* **68**, 1303–1321 (2017).
80. Risk, J. M., Laurie, R. E., Macknight, R. C. & Day, C. L. FRIGIDA and related proteins have a conserved central domain and family specific N- and C- terminal regions that are functionally important. *Plant Mol. Biol.* **73**, 493–505 (2010).
81. Zermiani, M. *et al.* Identification of the arabidopsis RAM/MOR signalling network: Adding new regulatory players in plant stem cell maintenance and cell polarization. *Ann. Bot.* **116**, 69–89 (2015).
82. Abraham-Juárez, M. J. *et al.* Evolutionary variation in MADS box dimerization affects floral development and protein abundance in maize. *Plant Cell* **32**, 3408–3424 (2020).
83. Wada, M. & Kong, S.-G. Actin-mediated movement of chloroplasts. *J. Cell Sci.* **131**, 210310 (2018).
84. Kodama, Y., Suetsugu, N., Kong, S.-G. & Wada, M. Two interacting coiled-coil proteins, WEB1 and PMI2 maintain the chloroplast photorelocation movement velocity in Arabidopsis. *Proc. Natl. Acad. Sci. U.S.A.* **107**, 19591–19596 (2010).
85. Zhang, X. & Liu, C.-J. Multifaceted regulations of gateway enzyme phenylalanine ammonia-lyase in the biosynthesis of phenylpropanoids. *Mol. Plant* **8**, 17–27 (2015).
86. Canella, D., Gilmour, S. J., Kuhn, L. A. & Thomashow, M. F. DNA binding by the Arabidopsis CBF1 transcription factor requires the PKKP/RAGR_xKFxETRHP signature sequence. *Biochim. Biophys. Acta* **1799**, 454–462 (2010).
87. Achard, P. *et al.* The cold-inducible CBF1 factor-dependent signaling pathway modulates the accumulation of the growth-repressing DELLA proteins via its effect on gibberellin metabolism. *Plant Cell* **20**, 2117–2129 (2008).
88. Cosgrove, D. J. Plant expansins: Diversity and interactions with plant cell walls. *Curr. Opin. Plant Biol.* **25**, 162–172 (2015).
89. Flint-Garcia, S. A., Thornsberry, J. M. & Buckler IV, E. S. Structure of linkage disequilibrium in plants. *Annu. Rev. Plant Biol.* **54**, 357–374 (2003).

90. Wilson, S. & Ruban, A. V. Rethinking the influence of chloroplast movements on non-photochemical quenching and photo-protection. *Plant Physiol.* **183**, 1213–1223 (2020).
91. Wada, M. Chloroplast movement. *Plant Sci.* **210**, 177–182 (2013).
92. Hüner, N. P. A. *et al.* Chloroplast redox imbalance governs phenotypic plasticity: The ‘grand design of photosynthesis’ revisited. *Front. Plant Sci.* **3**, 255 (2012).
93. Kitashova, A. *et al.* Impaired chloroplast positioning affects photosynthetic capacity and regulation of the central carbohydrate metabolism during cold acclimation. *Photosynth. Res.* **147**, 49–60 (2021).
94. Higa, T., Suetsugu, N., Kong, S.-G. & Wada, M. Actin-dependent plastid movement is required for motive force generation in directional nuclear movement in plants. *Proc. Natl. Acad. Sci. U.S.A.* **111**, 4327–4331 (2014).
95. Örvar, B. L., Sangwan, V., Omann, F. & Dhindsa, R. S. Early steps in cold sensing by plant cells: The role of actin cytoskeleton and membrane fluidity. *Plant J.* **23**, 785–794 (2000).
96. Uemura, M. *et al.* Responses of the plasma membrane to low temperatures. *Physiol. Plant.* **126**, 81–89 (2006).
97. Bredow, M. & Walker, V. K. Ice-binding proteins in plants. *Front. Plant Sci.* **8**, 2153 (2017).
98. Zhou, A. *et al.* PsCor413pm2, a plasma membrane-localized, cold-regulated protein from *Phlox subulata*, confers low temperature tolerance in *Arabidopsis*. *Int. J. Mol. Sci.* **19**, 2579 (2018).
99. Hahn, A. *et al.* Plant core environmental stress response genes are systemically coordinated during abiotic stresses. *Int. J. Mol. Sci.* **14**, 7617–7641 (2013).
100. Su, C. *et al.* Proteomic analysis of the function of a novel cold-regulated multispinning transmembrane protein COR413-PM1 in *Arabidopsis*. *Int. J. Mol. Sci.* **19**, 2572 (2018).
101. Houde, M. *et al.* Wheat EST resources for functional genomics of abiotic stress. *BMC Genomics* **7**, 149 (2006).
102. Zhang, C., Fei, S., Arora, R. & Hannapel, D. J. Ice recrystallization inhibition proteins of perennial ryegrass enhance freezing tolerance. *Planta* **232**, 155–164 (2010).
103. Dong, Z. *et al.* Maize LAZY1 mediates shoot gravitropism and inflorescence development through regulating auxin transport, auxin signaling, and light response. *Plant Physiol.* **163**, 1306–1322 (2013).
104. Campoli, C., Matus-Cádiz, M. A., Pozniak, C. J., Cattivelli, L. & Fowler, D. B. Comparative expression of *Cbf* genes in the *Triticeae* under different acclimation induction temperatures. *Mol. Genet. Genomics* **282**, 141–152 (2009).
105. Jung, W. J. & Seo, Y. W. Identification of novel *C-repeat binding factor (CBF)* genes in rye (*Secale cereale* L.) and expression studies. *Gene* **684**, 82–94 (2019).
106. Zhao, Y. *et al.* Dissecting the genetic architecture of frost tolerance in Central European winter wheat. *J. Exp. Bot.* **64**, 4453–4460 (2013).
107. Båga, M. *et al.* Identification of quantitative trait loci and associated candidate genes for low-temperature tolerance in cold-hardy winter wheat. *Funct. Integr. Genomics* **7**, 53–68 (2007).
108. Francia, E. *et al.* Two loci on chromosome 5H determine low-temperature tolerance in a ‘Nure’ (winter) × ‘Tremois’ (spring) barley map. *Theor. Appl. Genet.* **108**, 670–680 (2004).
109. Kanaoka, M. M. *et al.* SCREAM/ICE1 and SCREAM2 specify three cell-state transitional steps leading to *Arabidopsis* stomatal differentiation. *Plant Cell* **20**, 1775–1785 (2008).
110. Raissig, M. T., Abrash, E., Bettadapur, A., Vogel, J. P. & Bergmann, D. C. Grasses use an alternatively wired bHLH transcription factor network to establish stomatal identity. *Proc. Natl. Acad. Sci. U.S.A.* **113**, 8326–8331 (2016).
111. Hu, Y., Jiang, L., Wang, F. & Yu, D. Jasmonate regulates the inducer of *cbf* expression–*c-repeat binding factor/DRE binding factor1* cascade and freezing tolerance in *Arabidopsis*. *Plant Cell* **25**, 2907–2924 (2013).
112. Hibara, K.-I. *et al.* Jasmonate regulates juvenile-to-adult phase transition in rice. *Development* **143**, 3407–3416 (2016).
113. Osadchuk, K., Cheng, C.-L. & Irish, E. E. Jasmonic acid levels decline in advance of the transition to the adult phase in maize. *Plant Direct* **3**, 1–13 (2019).
114. Diallo, A. O. *et al.* Transcriptome analysis of an *mvp* mutant reveals important changes in global gene expression and a role for methyl jasmonate in vernalization and flowering in wheat. *J. Exp. Bot.* **65**, 2271–2286 (2014).
115. Shan, X., Zhang, Y., Peng, W., Wang, Z. & Xie, D. Molecular mechanism for jasmonate-induction of anthocyanin accumulation in *Arabidopsis*. *J. Exp. Bot.* **60**, 3849–3860 (2009).
116. Bahrani, H. *et al.* Preferential accumulation of glycosylated cyanidins in winter-hardy rye (*Secale cereale* L.) genotypes during cold acclimation. *Environ. Exp. Bot.* **164**, 203–212 (2019).
117. Yang, D.-L. *et al.* Plant hormone jasmonate prioritizes defense over growth by interfering with gibberellin signaling cascade. *Proc. Natl. Acad. Sci. U.S.A.* **109**, 1192–1200 (2012).
118. Li, G. *et al.* A high-quality genome assembly highlights rye genomic characteristics and agronomically important genes. *Nat. Genet.* **53**, 574–584 (2021).
119. Sandve, S. R. & Fjellheim, S. Did gene family expansions during the Eocene–Oligocene boundary climate cooling play a role in Pooidae adaptation to cool climates?. *Mol. Ecol.* **19**, 2075–2088 (2010).
120. Hanada, K., Zou, C., Lehti-Shiu, M. D., Shinozaki, K. & Shiu, S. H. Importance of lineage-specific expansion of plant tandem duplicates in the adaptive response to environmental stimuli. *Plant Physiol.* **148**, 993–1003 (2008).

Acknowledgements

Several research technicians and summer students over the last six years are acknowledged for help in the field and greenhouse work.

Author contributions

M.B.: Conceptualization, funding acquisition, experimental, data analysis, manuscript first draft preparation and editing. H.B.: Experimental, data analysis, manuscript writing. J.L.: Conceptualization, funding acquisition, resources, manuscript review. B.H.: Data analysis, manuscript review and editing. R.J.G.: Conceptualization, resources, manuscript review and editing. A.L.: Conceptualization, funding acquisition, data analysis, manuscript review and editing. R.N.C.: Conceptualization, funding acquisition, project management, data analysis, manuscript review and editing. All authors reviewed the manuscript and approved for publication.

Funding

This work was supported by the Canada Research Chairs (RNC), Natural Sciences and Engineering Research Council Canada (NSERC) Discovery grant (RNC), NSERC collaborative research project grant with Western Grains Research Foundation, Saskatchewan Winter Cereals Development Commission, Winter Cereals Manitoba Inc. and Alberta Wheat Commission, and a NSERC Alliance grant with Western Grains Research Foundation and Saskatchewan Winter Cereals Development Commission. HB is a grateful recipient of the Harvey scholarship and Devolved scholarship by the Department of Plant Sciences. BH was funding by the European Union’s

Horizon 2020 research and innovation programme under grant agreement No 771134 for the project RYE-SUS. RYE-SUS is carried out under the ERA-NET Cofund SusCrop (Grant No. 771134), being part of the Joint Programming Initiative on Agriculture, Food Security and Climate Change (FACCE-JPI).

Competing interests

The authors declare no competing interests.

Additional information

Supplementary Information The online version contains supplementary material available at <https://doi.org/10.1038/s41598-022-09582-2>.

Correspondence and requests for materials should be addressed to R.N.C.

Reprints and permissions information is available at www.nature.com/reprints.

Publisher's note Springer Nature remains neutral with regard to jurisdictional claims in published maps and institutional affiliations.



Open Access This article is licensed under a Creative Commons Attribution 4.0 International License, which permits use, sharing, adaptation, distribution and reproduction in any medium or format, as long as you give appropriate credit to the original author(s) and the source, provide a link to the Creative Commons licence, and indicate if changes were made. The images or other third party material in this article are included in the article's Creative Commons licence, unless indicated otherwise in a credit line to the material. If material is not included in the article's Creative Commons licence and your intended use is not permitted by statutory regulation or exceeds the permitted use, you will need to obtain permission directly from the copyright holder. To view a copy of this licence, visit <http://creativecommons.org/licenses/by/4.0/>.

© The Author(s) 2022